Twinning in an orthorhombic aluminate sodalite, $Ca_8[Al_{12}O_{24}](CrO_4)_2$

ISHMAEL HASSAN

Department of Geology, Faculty of Science, University of Kuwait, P.O. Box 5969, Safat, Kuwait 13060

Abstract

Transmission electron microscopy (TEM) was used to study the aluminate sodalite, $Ca_8[Al_{12}O_{24}](CrO_4)_2$. This aluminate sodalite has four polymorphs: one cubic, one modulated, one tetragonal, and an orthorhombic cell that arise from ordering of $[Ca_4{\cdot}CrO_4]^{6+}$ clusters that occur in the cages of the structure. The transition temperatures are 432, 453, and 610 K. The cell parameters for the orthorhombic phase, with the cubic cell parameter of $a = b = c = 9.222$ Å, are $3a \times 2b \times c$. Transformation twins are formed at 432 K during the transition from the tetragonal to the orthorhombic phase. The twin plane is {110} in the cubic cell, and {320} in the orthorhombic cell.

KEYWORDS: aluminate sodalite, twinning, sodalite group, nosean, haüyne, lazurite, TEM, superstructures.

Introduction

SYNTHETIC aluminate sodalites of general formula, $M_8[Al_{12}O_{24}](XO_4)_2$, with M = Ca, Sr, and X = S, Cr, Mo, W, form an interesting family of compounds. The most important reasons are: (1) the occurrence of ferroic phase transitions and the presence of ferroelectric and ferroelastic species; (2) the presence of modulated structures and superstructures; (3) the possible existence of tricritical points; (4) the occurrence of strong framework and cage atom interactions that cause important structural strains (bond length and angular; e.g. Depmeier *et al.*, 1987; Depmeier, 1988*a,b*).

Many materials have the sodalite, $Na_8[Al_6Si_6O_{24}]Cl_2$, structure (e.g. Hassan and Grundy, 1983, 1984, 1985, 1989, 1991*a,b*; Hassan *et al.*, 1985). The sodalite framework contains corner-linked TO_4 tetrahedra ($T = Si^{4+}$, Al^{3+}, Be^{2+}, B^{3+}, Ga^{3+}, and Ge^{4+}) and intervening large cavities, called cages in zeolite chemistry (Fig. 1). The cubo-octahedral cages are used as building blocks for many zeolites. The cations in the TO_4 tetrahedra are fully ordered in the different sodalite minerals. The structures are characterized by six-fold rings of TO_4 tetrahedra parallel to {111} planes in the cubic structure. These rings are stacked in a cubic ABCABC sequence. The structures are further characterized by four-fold rings of TO_4 tetrahedra parallel to {100} planes. The materials of interest here include the sulphatic aluminosilicate sodalites (nosean, haüyne, and lazurite) and the aluminate sodalites, in particular the aluminate sodalite $Ca_8[Al_{12}O_{24}](CrO_4)_2$.

The sulphatic aluminosilicate and aluminate sodalites that contain interstitial tetrahedral anion groups (e.g. SO_4^{2-}, CrO_4^{2-}, WO_4^{2-}, etc.) in the cages display complex satellite reflections in diffraction patterns. Details of satellite reflections from sulphatic sodalites differ for each mineral and differ among specimens, even from the same locality. Besides different chemistries, the satellite reflections are related to the temperature of formation of the minerals and the ordering processes that are associated with decreasing temperature (e.g. Saalfeld, 1961; Schulz, 1970; Taylor, 1967; Tsuchiya and Takeuchi, 1985; Hassan and Buseck, 1989*a,b*; Xu and Veblen, 1995). However, the origins of the satellite reflections are not known in detail.

The aluminate sodalites are stoichiometric, and the cage clusters (i.e. $[M_4{\cdot}XO_4]^{6+}$) are chemically identical and highly charged (6+ v.u.). Such highly charged clusters seem to stabilize Al-O-Al bonds, which are generally unstable in aluminosilicate minerals (see Hassan and Buseck, 1988). As the aluminate sodalite framework contains only Al atoms and these compounds are stoichiometric, the aluminate sodalite compounds are expected to be less complex structurally than the aluminosilicate sodalites. Thus, they may provide useful clues as to the origins of the satellite reflections in the sodalite-group

Mineralogical Magazine, August 1996, Vol. 60, pp. 617–622

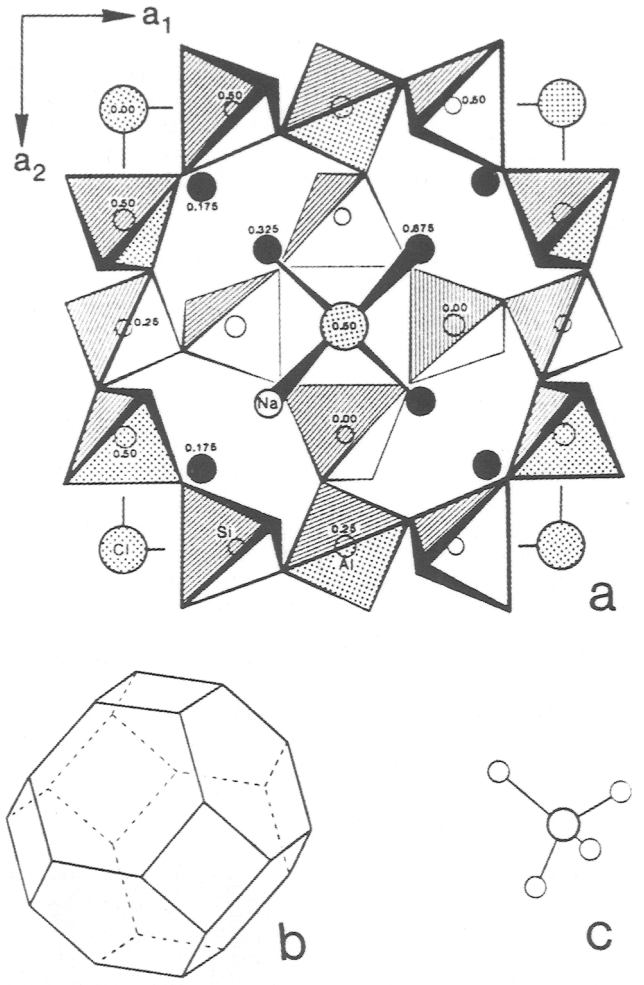

FIG. 1.(*a*) Crystal structure of sodalite. (*b*) Truncated cubo-octahedral cage in sodalite phases. (*c*) Cluster, e.g. $[Na_4{\cdot}Cl]^{3+}$, located in the centre of the cage.

minerals. However, difficulties with X-ray structure refinements of aluminate sodalites were met. According to Depmeier (1988*a,b*) the cubic high-temperature phases are characterized by disordered XO_4 groups over six orientational positions, and the transitions to the lower temperature tetragonal and orthorhombic phases are triggered by ordering of the XO_4 groups over fewer than six positions. The *M* atom is bonded to one or two O atoms of the XO_4 group. Therefore, there are essentially two geometrically different $[M_4{\cdot}XO_4]^{6+}$ clusters.

If the AlO_4 tetrahedra in the aluminate sodalites are regarded as regular and of equal sizes and the framework is fully expanded, the space group of the aluminate sodalites is *Im*3*m*. If the tetrahedra are rotated, the symmetry remains cubic, but the space group changes from *Im*3*m* to $I\bar{4}3m$. In the case of the aluminosilicate sodalites, the ordering of Al and Si atoms leads to a further reduction in symmetry to the cubic space group $P\bar{4}3n$ (see Hassan and Grundy, 1984).

Selected-area electron diffraction (SAED) patterns show that the $[Ca_4{\cdot}CrO_4]^{6+}$ aluminate sodalite has four polymorphs: one cubic, one modulated, one tetragonal, and an orthorhombic cell that arise from ordering of $[Ca_4{\cdot}CrO_4]^{6+}$ clusters (Hassan, 1994). The transition temperatures, *T*c, are 432, 453, and 610 K (Depmeier, 1988*a*). At high temperature ($\geqslant$610 K), the $[Ca_4{\cdot}CrO_4]^{6+}$ clusters in the cubic aluminate sodalite are disordered, together with the

framework oxygen atoms. As the temperature is lowered ($432 \leqslant T \leqslant 610$ K), the structure is modulated and the $[Ca_4 \cdot CrO_4]^{6+}$ clusters are ordered and accompanied by positional modulations of the framework oxygen atoms. Further ordering of the $[Ca_4 \cdot CrO_4]^{6+}$ clusters results in tetragonal ($432 \leqslant T \leqslant 453$ K) and orthorhombic (T<432 K) symmetries.

This paper reports on twinning in an aluminate sodalite. The material undergoes transitions from a cubic, to a modulated, to a tetragonal superstructure, and finally to an orthorhombic superstructure as the temperature is lowered. Transformation twins are formed during the transition from the tetragonal to the orthorhombic phase. The twins can be destroyed by heating the orthorhombic phase above the T_c of 432 K.

Electron microscopy

The aluminate sodalite used in this study is a synthetic sample (natural samples are unknown). The composition is $Ca_8[Al_{12}O_{24}](CrO_4)_2$, and the cubic cell parameter, a, is 9.222(2) Å. This aluminate sodalite has not been fully characterized by X-ray diffraction and the only reliable X-ray datum is the pseudocubic cell parameter (Depmeier, 1988*a*). Fragments of aluminate sodalite were obtained by crushing in acetone using an agate mortar and pestle. The crystals in suspension were deposited on holey carbon support films, and TEM data were recorded from thin regions. Electron microscopy was performed using various microscopes (JEOLs 200CX, 4000EX, and 1200EX 11).

Results

Superstructure cell parameters and directions in SAED patterns are reported with the cubic subcell parameter ($a = b = c = 9.222$ Å). Some crystal fragments of the aluminate sodalite contain reflections that indicate a supercell with parameters of $a \times 2b$ (Fig. 2). The s satellite reflections and streaks parallel to <110> are considered in a separate paper because they are not related to the twinning in the aluminate sodalite.

Supercell parameters of $2a \times 3b$ occur in other crystal fragments (Fig. 3). However, some reflections that are absent in some SAED patterns (Fig. 3*a*) do occur in others (Fig. 3*b*). A few extra reflections also occur, but they arise from adjacent regions of the same single-crystal fragment (Fig. 3*b*). An orthorhombic supercell with parameters of $3a \times 2b \times c$ can be used to uniquely index the above SAED patterns (Figs 2 and 3).

The aluminate sodalite gives some intriguing SAED patterns that arise from twinning (Fig. 4). These complex patterns can be explained by twinning of a $2a \times 3b$ supercell along a (110) plane. For example, Fig. 4*b* can be obtained from twinning of the $2a \times 3b$ supercell pattern shown in Fig. 3*b*. This can be seen by making two copies of Fig. 3*b* on transparencies, rotating one copy by 90° and placing it on the other; the resulting pattern is Fig. 4*b*. In fact, Figs 3*b* and 4*a*,*b* are from different areas of the same single-crystal fragment. Figure 4*a*, which shows an apparent $2a \times 6b$ supercell, can be obtained from the overlap of Figs 2 and 3*b*, which implies an interchange of the supercell ($3a \times 2b \times c$) edges (i.e. $3a$ for $2b$, and c for $2b$) during the growth of this single crystal.

Twinning can be seen in the [001] image of aluminate sodalite (Fig. 5), which corresponds with the SAED pattern given (Fig. 4*b*). The double-headed arrow points out the twin boundary, which is parallel to the (110) plane. Regions a and b have a twin relationship; both regions have $2a \times 3b$ supercells. The orientations of the twin components a and b and the supercell spacings are indicated on the image. The two parts of the crystal are intergrown so that all crystallographic directions of part a are related to the corresponding directions in part b by the operation of a mirror plane, which is parallel to a (110) plane. The twin in the aluminate sodalite is thus a reflection twin with (110) as both the compositional and the twin plane. The formation of the twins is associated with the transition from tetragonal to orthorhombic symmetry. The twins can be destroyed by heating the orthorhombic phase above the T_c of 432 K.

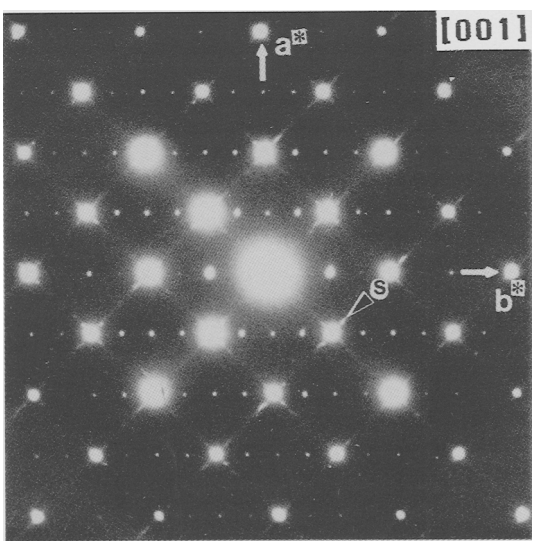

FIG. 2. [001] SAED pattern. The supercell is $a \times 2b$. The s satellite reflections and streaks occur along <110> (arrows).

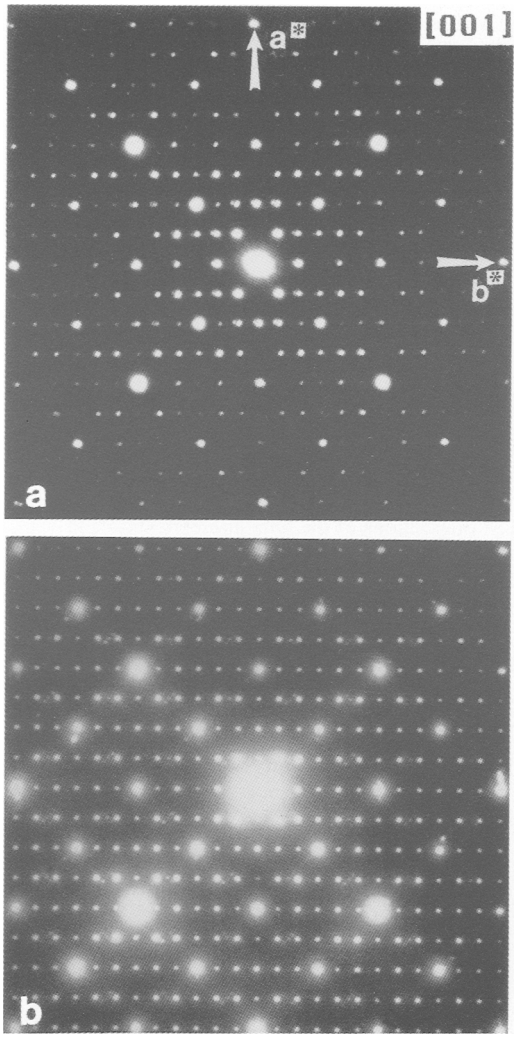

FIG 3. [001] SAED pattern. The supercell is $2a \times 3b$. Some reflections that are absent in (*a*) occur in (*b*). Both patterns have the same orientation and scale.

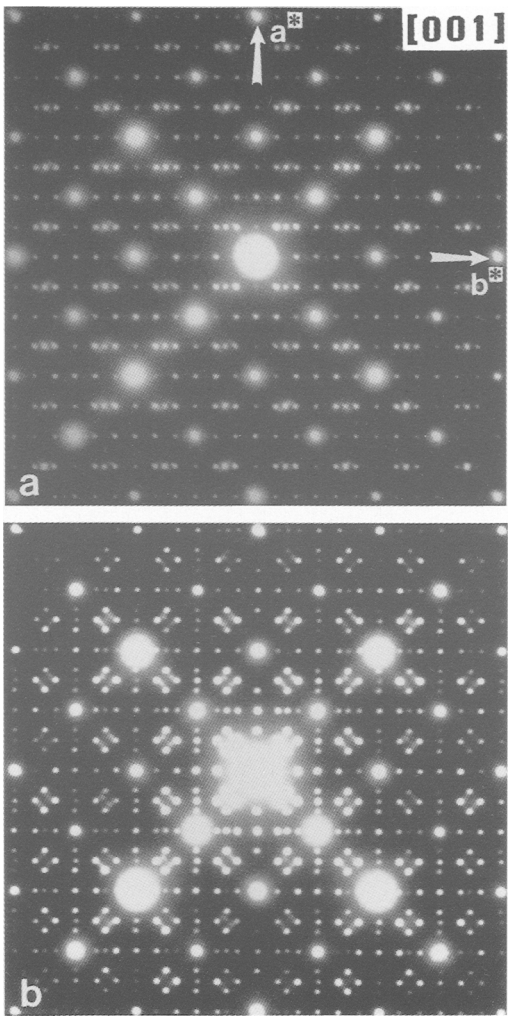

FIG. 4. Twinning in [001] SAED patterns of aluminate sodalite. A $2a \times 3b$ supercell is contained in both (*a*) and (*b*); these patterns are from different regions of the same single-crystal fragment. By twinning a $2a \times 3b$ supercell along a (110) plane, these patterns are obtained (see text). Both patterns have the same scale and orientation.

Discussion

Selected Area Electron Diffraction patterns show that the $[Ca_4{\cdot}CrO_4]^{6+}$ aluminate sodalite has four polymorphs: one cubic, one modulated, one tetragonal, and an orthorhombic cell that arise from ordering of $[Ca_4{\cdot}CrO_4]^{6+}$ clusters (Hassan, 1994). The transition temperatures, T_c, are 432, 453 and 610 K (Depmeier, 1988*a*). The cell parameters for the orthorhombic phase, with the cubic cell parameter of $a = b = c =$ 9.222 Å, are $3a \times 2b \times c$ (this study).

Aluminate sodalite crystals are almost inevitably twinned because the temperatures of crystal growth are higher than the temperatures of the phase transitions. Depending on the type of symmetry element lost, the phase transition may result in the formation of twin domains in the case of transitions comprising supergroup-subgroup relations. Merohedral and pseudomerohedral twinning may

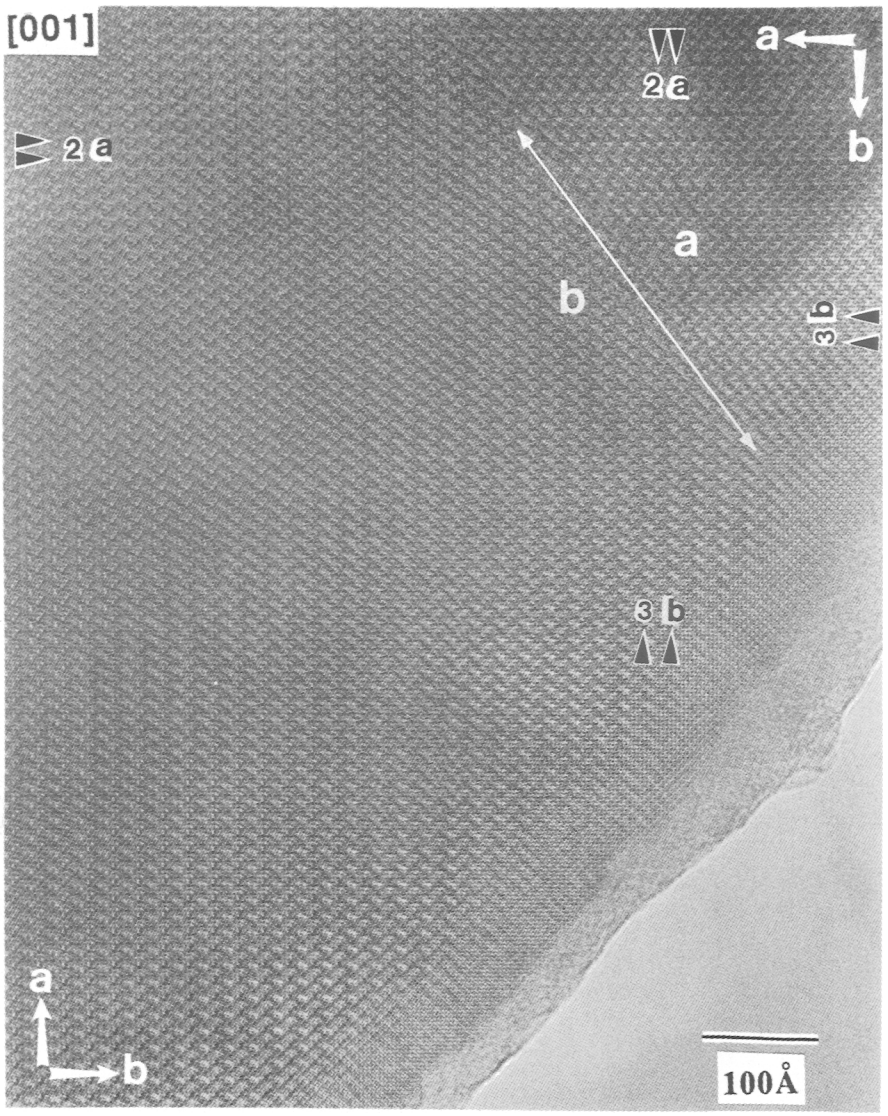

FIG. 5. Twinning in the [001] image of aluminate sodalite. The double-headed arrow points out the twin boundary, which is parallel to the (110) plane. Regions a and b have a twin relationship: both regions have a $2a \times 3b$ supercell.

occur simultaneously in all aluminate sodalites (see Depmeier, 1988*a*).

Twinning has been reported for $[Ca_4 \cdot WO_4]^{6+}$ aluminate sodalite, which has space group *A*ba2 and supercell parameters of $2(a + b) \times (a - b) \times c$ (i.e. 26.123, 13.066, and 9.319 Å; Depmeier, 1984). The twin plane in the cubic (or tetragonal) cell is {110}, and is {100} in the orthorhombic cell. The {100} was reported as {210} by Depmeier (1984). Because |a| = 2|b|, the twinning results in apparent equivalent axes a′ = b′ and, thus, in apparent tetragonal symmetry, provided that the intensity contributions of the two twin individuals are equal (Depmeier, 1984).

During the transition from the tetragonal to the orthorhombic phase, transformation twins are formed. Twinning was observed only in the orthorhombic phase. The twin plane is {110} for the cubic cell, and {320} for the orthorhombic cell. This twinning interchanges the 3*a* and 2*b* axes (Fig.

3*b*). Other axes can also be interchanged during the growth of a single crystal. For example, the cell edges such as *c* and 2*b*, and 2*b* and 3*a* are interchanged during crystal growth to give Fig. 4*a*, which is a combination of the $c \times 2b$ and $2b \times 3a$ repeats (i.e. overlap of Figs 2 and 3*b*). This implies that all {110} planes are possible twin planes in the cubic cell. These results for $[Ca_4{\cdot}CrO_4]^{6+}$ aluminate sodalite are different from those reported for $[Ca_4{\cdot}WO_4]^{6+}$ aluminate sodalite using X-ray diffraction techniques (see Depmeier, 1984). The results are different in terms of both cell parameters and twin planes for the two different aluminate sodalites.

Conclusions

The aluminate sodalite has four polymorphs: one cubic, one modulated, one tetragonal and an orthorhombic cell. The transition temperatures, T_c, are 432, 453, and 610 K. Twinning occurs only in the orthorhombic phase.

During the transition from the tetragonal to the orthorhombic phase at 432 K, transformation twins are formed. The twins can be destroyed by heating the orthorhombic phase above the T_c of 432 K. The twin plane is {110} in the cubic cell, and is {320} in the orthorhombic cell. In the cubic cell, all {110} planes are possible twin planes and twinning does occur on them.

Acknowledgements

Dr John Barry is thanked for useful discussions and for his help in using the 4000EX microscope. The aluminate sodalite sample was provided by Dr Yohan DeVellier. An anonymous reviewer and the Associate Editor, Dr P. E. Champness, are thanked for useful comments on this manuscript. This work was financially supported by a University of Kuwait grant SG-038 and by a NSF grant EAR-8708169 to Dr Peter R. Buseck, who is thanked for his support and encouragement; microscopy data were obtained at Arizona State University HREM Facility and at the University of Kuwait EM Centre.

References

Depmeier, W. (1984) Aluminate sodalite $Ca_8[Al_{12}O_{24}](WO_4)_2$ at room temperature. *Acta Crystallogr.*, **C40**, 226–31.

Depmeier, W. (1988*a*) Aluminate sodalites — a family with strained structure and ferroic phase transitions. *Phys. Chem. Minerals*, **15**, 419–26.

Depmeier, W. (1988*b*) Structure of cubic aluminate sodalite $Ca_8[Al_{12}O_{24}](WO_4)_2$ in comparison with its orthorhombic phase and with cubic $Sr_8[Al_{12}O_{24}](CrO_4)_2$. *Acta Crystallogr.*, **B44**, 201–7.

Depmeier, W., Schmid, H., Setter, N. and Werk, M.L. (1987) Structure of cubic aluminate sodalite $Sr_8[Al_{12}O_{24}](CrO_4)_2$. *Acta Crystallogr.*, **C43**, 2251–5.

Hassan, I. (1994) The crystal chemistry of the feldspathoids and their relationship to the zeolites. *IMA Abstracts with Program*, Pisa, Italy, **16**, 695.

Hassan, I. and Buseck, P.R. (1988) A HRTEM characterization of scapolite solid-solutions. *Amer. Mineral.*, **73**, 119–34.

Hassan, I. and Buseck, P.R. (1989*a*) Incommensurate-modulated structure of nosean, a sodalite-group mineral. *Amer. Mineral.*, **74**, 394–410.

Hassan, I. and Buseck, P.R. (1989*b*) Cluster ordering and antiphase domain boudaries in hauyne. *Canad. Mineral.*, **27**, 173–80.

Hassan, I. and Grundy, H.D. (1983) Structure of basic sodalite, $Na_8Al_6Si_6O_{24}(OH)_2{\cdot}2H_2O$. *Acta Crystallogr.*, **C39**, 3–5.

Hassan, I. and Grundy, H.D. (1984) The crystal structures of sodalite-group minerals. *Acta Crystallogr.*, **B40**, 6–13.

Hassan, I. and Grundy, H.D. (1985) The crystal structure of helvite group minerals, $(Mn,Fe,Zn)_8(Be_6Si_6O_{24})S_2$. *Amer. Mineral.*, **70**, 186–92.

Hassan, I. and Grundy, H.D. (1989) The structure of nosean, ideally $Na_8[Al_6Si_6O_{24}]SO_4{\cdot}H_2O$. *Canad. Mineral.*, **27**, 165–72.

Hassan, I. and Grundy, H.D. (1991*a*) The crustal structure of hauyne at 293 and 153 K. *Canad. Mineral.*, **29**, 123–30.

Hassan, I. and Grundy, H.D. (1991*b*) The crystal structure and thermal expansion of tugtupite, $Na_8(Al_2Be_2Si_8O_{24})Cl_2$. *Canad. Mineral.*, **29**, 385–90.

Hassan, I., Peterson, R.C. and Grundy, H.D. (1985) The structure of lazurite, ideally $Na_6Ca_2(Al_6Si_6O_{24})S_2$, a member of the sodalite group. *Acta Crystallogr.*, **C41**, 827–32.

Saalfeld, H. (1961) Strukturbesonderheiten des Hauyngitters. *Z. Krist.*, **115**, 132–40.

Schulz, H. (1970) Struktur und Uberstukturunter-suchungen an Nosean-Einkristallen. *Z. Krist.*, **131**, 114–38.

Taylor, D. (1967) The sodalite group of minerals. *Contrib. Mineral. Petrol.*, **16**, 172–88.

Tsichiya, N. and Takéuchi, Y. (1985) Fine texture of hauyne having a modulated structure. *Z. Krist.*, **173**, 273–81.

Xu, H. and Veblen, D.R. (1995) Transmission electron microscopy study of optically anisotropic and isotropic haüyne. *Amer. Mineral.*, **80**, 87–93.

[*Manuscript received 1 June 1995: revised 12 October 1995*]